



# Solidification of an Al-Zn alloy during semi-solid processing

by S.L. George\* and R.D. Knutsen\*

## Synopsis

The semi-solid metal casting process results in a unique solidification path. The microstructural features that were identified during the characterization of the as-cast microstructure, were used as evidence of the process history in order to determine the solidification path followed during the evolution of the microstructure. The morphology of the grains was characterized using SEM and the extent and distribution of the elemental segregation within the grain structure was analysed using EDS.

## Keywords

Semi-solid casting, solidification path, segregation.

## Introduction

Semi-solid metal (SSM) casting is a relatively new manufacturing route which offers an attractive near-net shape manufacturing route for precipitation hardenable aluminium alloy components, potentially giving them mechanical properties that are comparable to a wrought or machined equivalent product, but with the benefit of the rapid processing route of casting.

The key to the potential for high strength using the SSM casting technique is the as-cast microstructure that develops as a result of the production process. The SSM microstructure differs from the dendritic microstructure that is associated with traditional casting, in that it consists of a globular grain morphology that originates from the turbulent mixing that is a characteristic step forming part of the semi-solid slurry production process<sup>1</sup>. The mechanisms involved during agitation in the slurry production step lead to the formation of globular solid particles within the melt. These particles continue to form and the slurry is transferred to the high pressure die casting facility when it reaches a solid fraction of approximately 50%. The mechanisms causing the globularization of the slurry have an effect on the nature of the final  $\alpha$ -primary globular particles and, hence, affect the evolution of the as-cast structure during any post solidification heat treatments.

Research into SSM processing and the resulting globular microstructure and the mechanisms that make it so, has been on-going for more than 30 years. Over this time, various researchers have used different analysis techniques and have come to varying conclusions as to the true mechanism behind the morphological changes that occur during stirring. These can be divided into two general categories: dendrite deformation and spherical growth<sup>2,3</sup>. Within each of these categories there are various theories that claim to explain the globularization mechanisms. The deformation theories are based on the growth mode at the solid-liquid interface being dendritic, thereafter the mechanisms are described as either resulting in fragmentation<sup>4-6</sup> or deformation by bending<sup>7</sup> of the dendrite arms as a result of the shear stresses experienced during stirring.

More recently theories involving spherical or cellular growth<sup>8</sup> at the interface have been proposed as more likely mechanisms.

The microstructural characteristics, defined by the grain size and distribution, the segregation and other key features, are evidence of the process history of the part. Therefore, by analysing the data obtained from a full characterization process, the microstructural evidence alludes to the mechanisms and kinetics involved following the path of solidification during SSM casting, from initial growth of solid nuclei within the melt, through the slurry production stage, the cessation of stirring for the transfer of the slurry to the HPDC facility, the casting, and finally the solid state cooling. The current study looks at the evolution of the globular microstructure and

\* Centre for Materials Engineering, Mechanical Engineering, University of Cape Town, Cape Town.

© The Southern African Institute of Mining and Metallurgy, 2011. SA ISSN 0038-223X/3.00 + 0.00. This paper was first presented at the, Light Metals Conference, 27-29 October 2010, Misty Hills, Muldersdrift.

## Solidification of an Al-Zn alloy during semi-solid processing

the associated elemental segregation, by following the solidification path experienced during SSM casting. By mapping the evolution of the SSM cast microstructure, it is hoped that, ultimately, resolutions may be obtained for the removal of the extensive segregation within semi-solid cast structures by way of the development of successful homogenization and heat treatment practices.

### Experimental approach

The alloys under investigation were an AA7075 composition alloy and a custom-made A713 composition alloy. The compositions are shown in Table I.

The samples were supplied by the Council for Scientific and Industrial Research (CSIR) in Pretoria, South Africa. The samples underwent a controlled cooling and stirring stage in the CSIR rheocasting facility prior to casting in a 50 ton high pressure die casting (HPDC). The final plates were 100 mm x 60 mm x 4 mm. Samples were sectioned from the centre of each plate for evaluation. Each sample was mounted and polished to a mirror finish using colloidal silica for microstructural evaluation. For low magnifications, polarized light optical microscopy (PLOM) was used. In these cases the samples were electro-anodized using a 2% HBF<sub>4</sub> Barkers solution. During anodizing the applied electrical field produces a thick oxide layer on the surface of aluminium sample. When the sample is viewed in cross-polarized light during PLOM, the interference of light as a result of the oxide layer produces colours, which depend on the grain orientation

below the oxide layer. Thus grains of different orientation within a micrograph will be viewed as different colours. The colour differences are relative to neighbouring grains and do not offer quantitative information about crystal orientation.

SEM imaging in conjunction with energy dispersive X-ray spectroscopy (EDS) and electron backscatter diffraction (EBSD) was used to fully characterize the as-cast microstructure. Focus was placed on determining the location, extent and distribution of the elemental segregation within the structure, as well as quantitative orientation information attained from EBSD mapping. These techniques were used to identify the features that aid in the interpretation of the path followed during solidification.

### Results and discussion

PLOM micrographs revealed a globular grain structure with a relatively homogeneous distribution of grains. The globular grains were orientated at random within the structure. The general as-cast microstructure can be seen in Figure 1(a). The microstructure is more clearly defined at higher magnification in the SEM image in Figure 1(b) where the contrast provided by the backscattered electron (BSE) detection highlights the elemental differences within the as-cast microstructure. The relative compositions of the main alloying elements, aluminium and zinc, were determined using an EDS linescan across the grain shown in Figure 1(b). It can be seen that, although the composition is fairly uniform

Table I

Chemical composition (in wt%) of the Al-Zn alloys used in this investigation

	Zn	Mg	Cu	Fe	Si	Cr	Mn	Al
AA7075	5.56	2.45	1.55	0.24	0.24	0.18	0.15	balance
AA7075*	5.1–6.1	2.1–2.9	1.2–2.0	0.50	0.40	0.18–0.28	0.30	balance
A713	7.62	0.52	2.58	0.26	0.31	---	0.03	balance
A713**	7.6	0.4	0.8	0.55	0.12	0.06	0.2	balance

\* Alcoa standard for AA7075 wrought alloy  
 \*\* Alcoa standard for A713 casting alloy

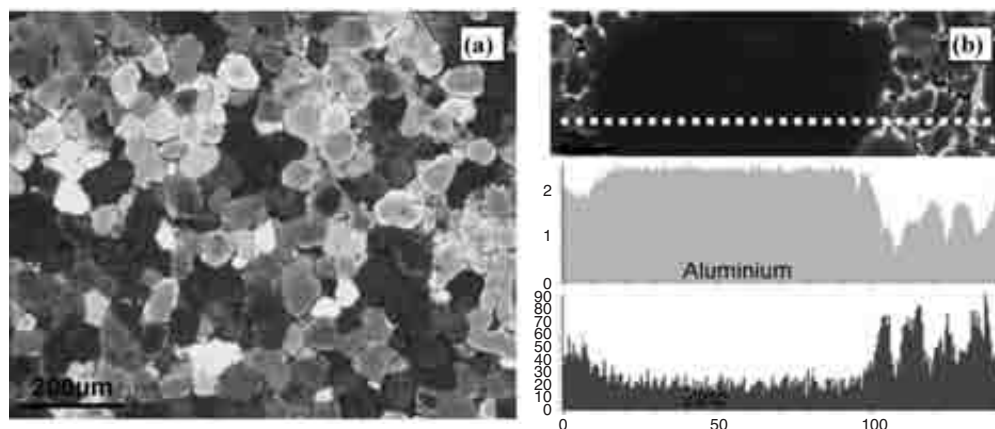


Figure 1—(a) PLOM image of SSM cast AA7075 composition alloy and (b) SEM backscattered electron image at a higher magnification with EDS linescans showing the relative compositions of Al and Zn across the grain (location of scan indicated by the dotted line)

## Solidification of an Al-Zn alloy during semi-solid processing

at the centre of the grain, the zinc content increased and the aluminium content decreases in a band at the edges of the grain, indicating the presence of a coring ring. The main contrast is seen between the large primary globular grains and the solute rich eutectic phases between the smaller grains in the interglobular regions. EDS spot analysis of the grains in the SSM cast AA7075 composition alloys revealed that the composition of the main alloying elements at the centre of the globular grains was approximately 93wt% Al and 4wt% Zn. The EDS values are considered qualitatively for the purpose of comparison, as the errors to the values owing to sample interaction volume were not included. The EDS composition values were constant for the central area of the grain (indicated by the EDS elemental concentration curves in Figure 1 (b)). At the outer edges of the globular grains the composition changes and the contrast in the BSE images shows a coring ring. The composition in this area shows a gradual decrease in Al and corresponding increase in Zn as the edge of the grain approaches. EDS results show that the composition at the edge of the band is generally of the order of 84wt% Al and 13wt% Zn. The composition of the solute rich areas between the grains is approximately 43wt% Al, 30wt% Zn and 14wt% Mg, indicating that the phases present in this region are  $\alpha$ -Al and  $MgZn_2$ .

The outer edges of the grains exhibit cellular protrusions which extend from the outer edge of the coring ring into the interglobular regions. The presence of these protrusions is seen where the growth of the grains is not impinged by the growth front of neighbouring grains. The protrusions can be seen in more detail in the EBSD maps in Figure 2. The different shades of grey in the EBSD map in Figure 2(b) indicate the different crystal orientations of the grains and the boundaries between neighbouring grains, or areas of different orientation, are shown as black lines, in the case of high angle grain boundaries (HAGBs) and light grey lines, in the case of low angle grain boundaries (LAGBs). The light grey regions between the grains in Figure 2(b) (corresponding to the black regions in Figure 2(a)) are un-indexed data points. The cellular protrusions have the same orientations as the grains from which they extend. The EBSD orientation map in Figure 2(b) also shows that the centre of the grain in the bottom right-hand corner of the map contains

strain and dislocation at the centre of the globular grain (the strain induced grain boundaries are indicated by the arrow in Figure 2(b)), with a strain-free region which coincides with the coring ring (indicated by the area between the dotted lines in the image in Figure 2(b)) seen in Figure 1 (b).

The features and composition variations seen in the microstructure show that there are distinct growth stages that occur during SSM casting, and that the solidification path that is followed is that of a multistage solidification process that deviates considerably from that of the conventional solidification of alloys. Using the microstructural and compositional information and the casting parameters, a schematic representation of the temperature-time profile for solidification can be drawn. This can be seen in Figure 3.

There are four stages of growth after nucleation. The first stage of growth occurs immediately after nucleation, at the onset of the stirring during slurry production. Growth is initially cellular.

The second stage of growth occurs during the highly turbulent stirring stage, where the collision rate is high and there is a constant fluctuation of stable and unstable growth at the solid-liquid interface. When the interface is unstable, cellular protrusions form and as the interface again approaches planar growth owing to the turbulence, the protrusions are removed. The net growth of the solid is planar at the end of the slurry production stage and the slurry is transferred to the HPDC machine when the solid fraction of globular particles within the melt reaches approximately 50%. If the shear forces experienced during stirring were insufficient to retard dendritic growth, this stage would comprise of deformation of the dendrite arms.

The third stage of growth occurs once the stirring has ceased. The solid-liquid interface is still planar, but there is a change in the composition of the new solid that forms as the liquid no longer experiences complete mixing and a resulting concentration gradient is seen in the form of a coring ring.

The final growth stage occurs during the mould-filling and solidification within the die during HPDC. The growth of the cellular protrusions at the unstable solid-liquid interface are unconstrained and they continue to grow until they impinge on neighbouring grains, be it either large globular grains or smaller interglobular grains. Further segregation is seen along the length of these protrusions.

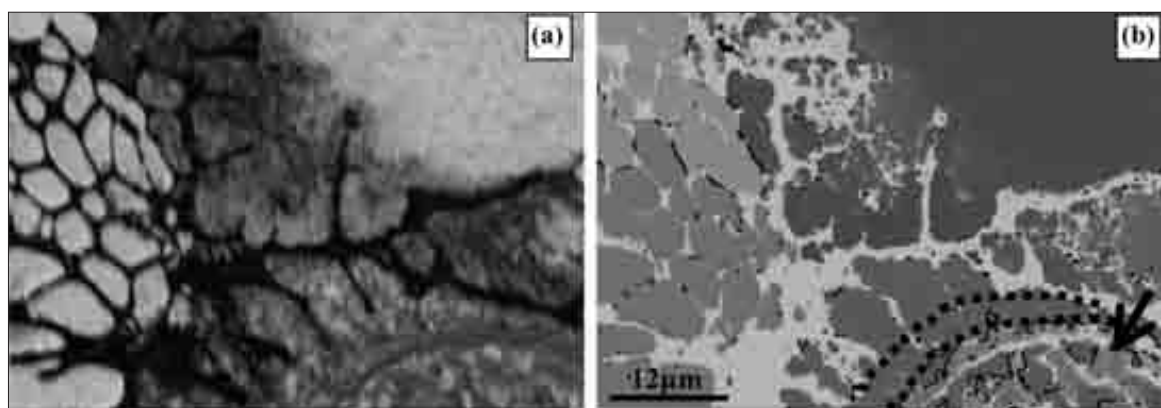


Figure 2—(a) EBSD band contrast image and (b) EBSD orientation map of SSM as-cast AA7075 composition alloy

## Solidification of an Al-Zn alloy during semi-solid processing

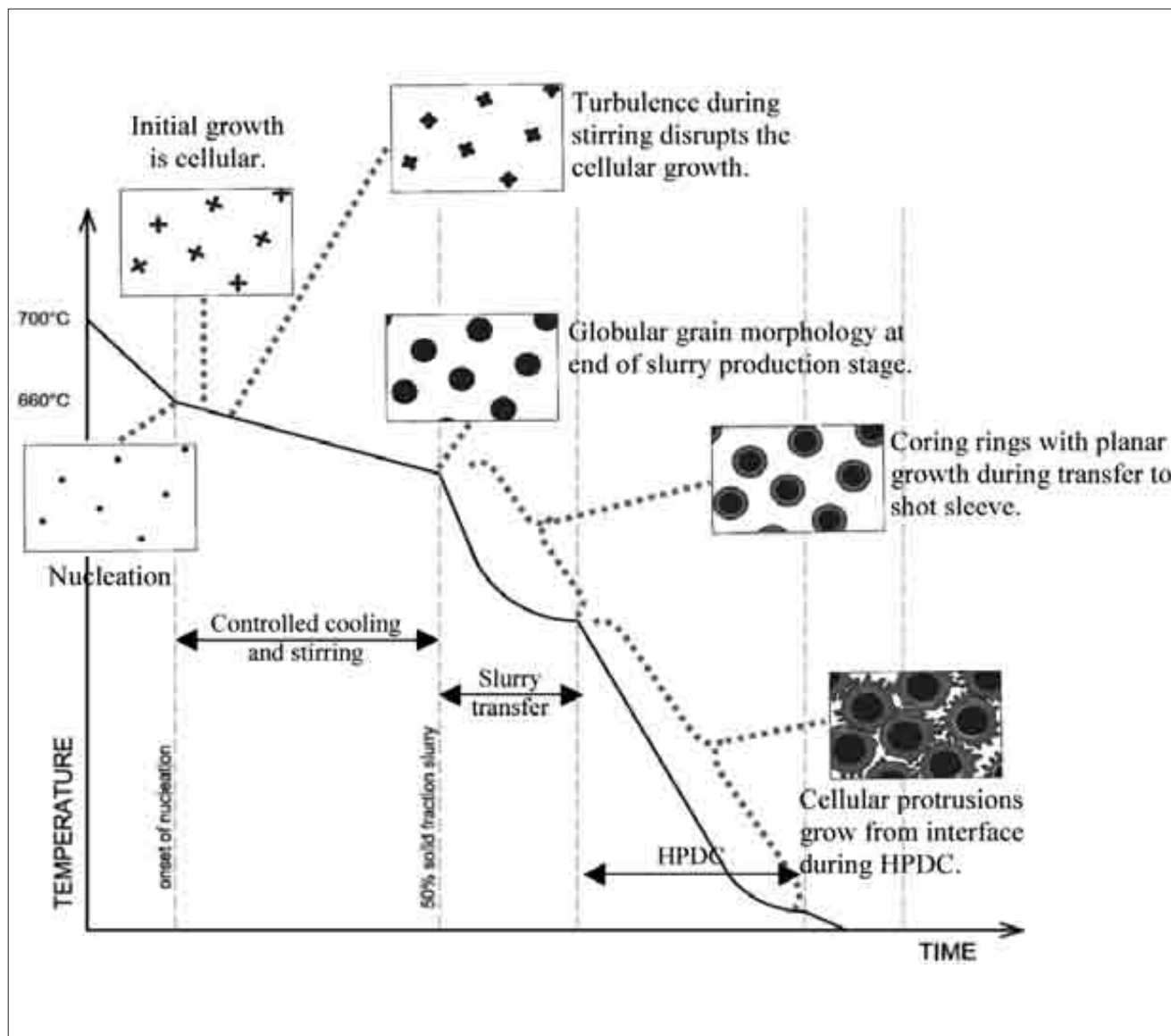


Figure 3—Solidification progression curve, with schematic diagrams indicating the microstructural evolution

The solidification path and the four main growth stages result in distinct areas of segregation. The high degree of segregation within the SSM as-cast structure will adversely affect the ability to precipitation harden the part during any post-solidification heat treatments. For this reason, knowledge of the solidification path is necessary for the understanding of the extent of the segregation in order to determine the homogenization processes necessary to remove the segregation prior to age hardening.

### Conclusions

The SSM casting process results in a unique solidification path, comprising four distinct growth stages. The path determines the location and extent of the micro-segregation within the as-cast structure. There is a high degree of elemental segregation associated with the SSM cast structure, located in the coring rings and cellular protrusions. The remaining solute is located in the interglobular region as eutectic phases.

### References

- CZERWINSKI, F. The basics of modern SSM processing, *Journal of Metals* (JOM), vol. 58, no. 6, June 2006, pp. 17–20.
- FAN, Z. and LUI, G. Solidification behaviour of AZ91D alloy under intensive forced convection in the RDC process, *Acta Materialia*, vol. 53, 2005, pp. 4345–4357.
- FAN, Z. Semi-solid metal processing, *International Materials Review*, vol. 47, no. 2, 2002, pp. 1–37.
- FLEMINGS, M.C. Behavior of metal alloys in the semisolid state, *Metallurgical Transactions A*, vol. 22A, May 1991, pp. 957–981.
- VOGEL, A., DOHERTY, R.D., and CANTOR, B. Stir-cast microstructure and slow crack growth, *Solidification and Casting of Metals: Proceedings of an international conference on solidification*, Sheffield Metallurgical and Engineering Association, University of Sheffield, 1977, pp. 518–525.
- DOHERTY, R.D., LEE, H.-L., and FEEST, E.A. Microstructure of stir-cast metals, *Materials Science and Engineering*, vol. 65, 1984, pp. 181–189.
- MULLIS, A.M. Growth induced dendritic bending and rosette formation during solidification in a shearing flow, *Acta Materialia*, vol. 47, no. 6, 1999, pp. 1783–1789.
- MOLENAAR, J.M.M., SALEMANS, F.W.H.C., and KATGERMAN, L. The structure of stircast Al-6Cu, *Journal of Materials Science*, vol. 20, 1985, pp. 4335–4344. ◆